Internal circulations inside the liquid slugs of liquid-liquid slug flow capillary microreactor

M. N. Kashid[1,2], J. F. Acker[2], F. Platte[1,2], D. W. Agar[1] and S. Turek[2,*]

[1] Institute of Reaction Engineering, University of Dortmund, 44227 Dortmund, Germany.

[2] Institute for Applied Mathematics, University of Dortmund, 44227 Dortmund, Germany.

Abstract

For mass transfer limited liquid-liquid reactions, a so called "slug flow" capillary microreactor has already been suggested. Internal circulations inside the slugs lead to increased mass transfer. The knowledge on the development of circulations and effects of operating parameters is crucial. The present work shows the state of art to predict the internal circulation inside the liquid slugs using computational fluid dynamics (CFD) simulations and visualization with the help of developed CFD particle tracing algorithm. Each slug was considered as separate domain and solved for individual slug as single phase flow. The effect of flow velocity and slug length on the velocity profile, stagnant region and internal circulations for slug without and with film is discussed. The internal circulations were qualitatively predicted with the help of particle tracing algorithm.

Keywords: Slug Flow, CFD, Internal Recirculations, Particle Tracing

* Author to whom correspondence should be addressed
Email Address: Stefan.Turek@math.uni-dortmund.de
Tel: +49 231 755 3075. Fax: +49 231 755 5933

Introduction

Microreactor technology, a key activity of process intensification, is expected to have a number of advantages in the process industries. Liquid-liquid reactions exhibiting mass transfer limitations are gaining more importance in small scale reactors like liquid-liquid slug flow microreactors (see Burn & Ramshaw, 1999). In this type of reactor, both phases move with constant slug volume and well defined mass transfer area. There are two ways of mass transfer, convection inside the liquid slug and diffusion between two slugs. The mass transfer is enhanced by internal circulation due to the shear between continuous phase/wall surface and slug axis, which leads to reduced path length and higher reaction rate. Strongly exothermic and hazardous reactions can be controlled with more precision, which can possibly give the technical relevance in the design of reactors for large scale production. In these reactors, the important parameters are pressure drop, selectivity and experimental stability of slug flow and wall film. In addition to this, internal flow patterns inside the slug plays important role in deciding the performance of the reactor.

Packed bed microreactor for temporal analysis of products was used by Zou et al. (1993) to illustrate the effect of pulse inlet using measured mass spectrometer response of the reactant and quantified the results with developed model. Then several studies were made on hydrodynamics to identify the flow regime and flow regime transition by experimental characterization and modeling of the gas-liquid flows through different micro-systems (Paglianti et al; 1996, Mishima & Hibiki; 1996, Triplett et al; 1999; Kreutzer 2003 and Simmons et al; 2003). Dispersion and mass transfer studies for gas-liquid flows are also available (Thulasidas et al; 1995, Bercic & Pinter; 1997 and Elperin & Fominykh; 1998). The flow patterns in the liquid slugs inside the capillaries were determined by Thulasidas et al. (1997) using particle imaging velocimetry (PIV) and reported recirculating patterns with high

degree of mixing. Few studies (like Piarah et al; 2001, Waheed et al; 2002 and Bothe et al; 2003) on mass transfer from drops and bubbles to the surrounding fluid have given the numerical methodologies to predict the mass transfer. Recently, Taha and Cui (2004) used volume of fluid CFD method to obtain the velocity and bubble profile inside the vertical gas-liquid slug flow inside the capillaries and found good agreement with published experimental measurements.

The application of slug (capsules) in transportation of oil was studied experimentally by Hodgson and Charles (1963) and reported flow regimes, slug velocity and pressure gradient in oil-water flow through a 1.04 inch internal diameter horizontal pipe. They revealed from the actual photographs of flow patterns that the viscous or semi-rigid oil phase is completely surrounded by much less viscous water. Further, Charles (1963) developed a model for measurement of slug velocity and pressure gradient for laminar and turbulent flow conditions. The major contribution in the use of liquid-liquid slug flow in microreactors is done by Professor Ramshaw's group from University of Newcastle, UK. Their experimental work of immiscible liquid-liquid flow inside a narrow channel for nitration of benzene shows the industrially competitive reaction rates (Burns & Ramshaw; 1999). In 2001, they developed a multiphase microreactor based upon the use of liquid-liquid slug flow and obtained mass transfer performance data for extraction of acetic acid from kerosene slugs. Based on their proposed device, Dummann et al. (2003) carried out experiments for the production of nitrobenzene in a capillary microreactor. The reaction was carried out in slug flow regime and it was observed that there was formation of by-products. They have done some CFD simulations and concluded that the enhancement of mass transfer can be interpreted in terms of an internal circulation flow within the plugs. Recently, Harries et al. (2003) developed a numerical model to simulate the segmented liquid-liquid flow. The general purpose CFD code

was extended in order to predict the internal flow patterns of fluid segments and the transfer of dissolved chemical species within segments and across fluid segment interfaces.

From the literature review it is cleat that there is no model or methodology available which can give better understanding on the effect of operating parameters on the internal circulations inside the liquid slugs of liquid-liquid slug flow capillary microreactor. CFD could be one of the important methodologies which can give better understanding and quantitative information about flow patterns over wide operating window. In this present work, an attempt has been made to study the effect of film and other operating parameters like flow velocity and slug length on internal circulations inside the liquid slug using CFD. The simulations were carried out using the experimental operating conditions from Dummann et al. (2003). The stagnation region and circulation time was calculated from simulated results. For better physical understanding and visualization, a CFD particle tracing algorithm was developed.

Internal Circulations

When slugs move through the capillary, depending on the physical properties and operating conditions, internal circulations inside the slugs take place. The liquid inside the slug is driven by the wall surface and slug axis, which produce internal circulations. In many studies, it was revealed that there was wall film formation by one phase (continuous phase) on both sides of the other phase (discrete phase). In this case the liquid inside the slug is driven by the outer flow of film and slug through the interface. These circulations inside the slug reduce the thickness of boundary layer like interface between two fluids and wall film. In the presence of film, the whole slug surface take part in the mass transfer however if there is no film only ends of the slug take part. Thus the interfacial area for mass transfer between two phase

increases due to film thereby increases the mass transfer. This film thickness can be calculated the Bretherton law (Bico & Quere; 2000):

$$h = 1.34RCa^{2/3} \quad (1)$$

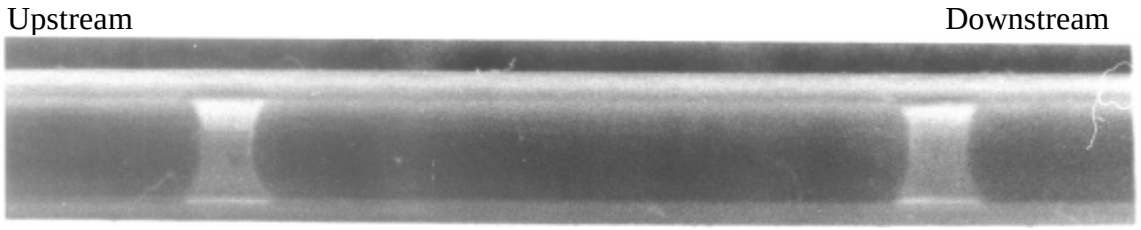

Figure 1a: Liquid-liquid slug flow in a capillary millireactor showing stained aqueous phase and colourless organic phase (Dummann et al., 2003)

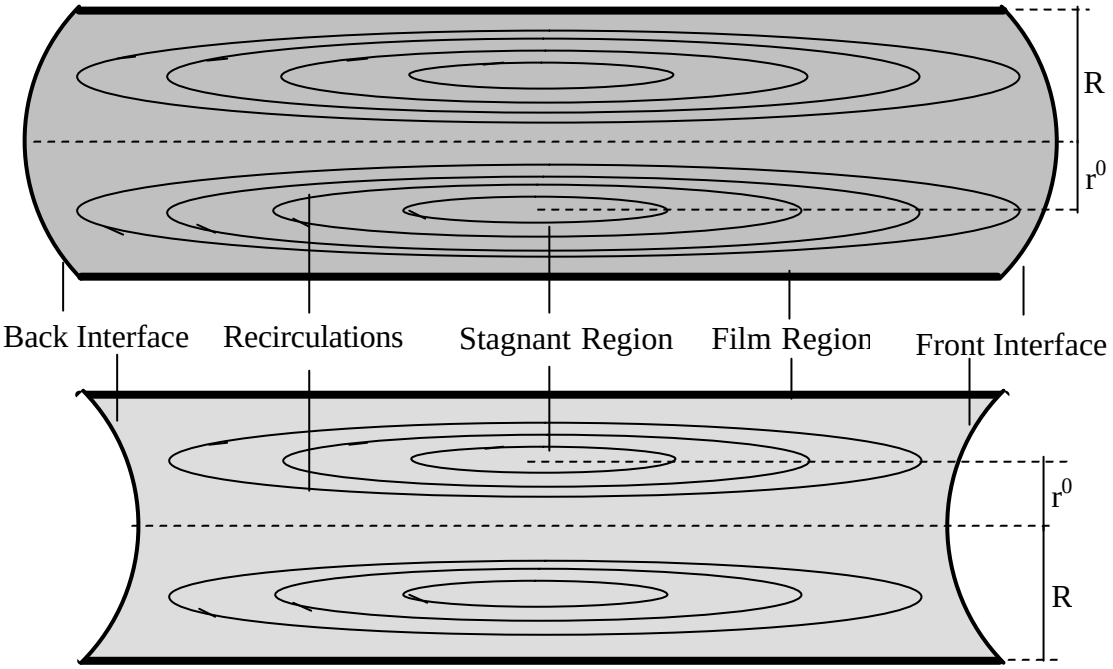

Figure 1b: Schematic representation of internal circulations inside the aqueous and organic slug respectively.

Dummann et al. (2003) used aqueous (mixture of concentrated sulphuric and nitric acid) and organic (benzene) phases for the production of nitrobenzene are shown in Figure 1a. The schematic representation of internal circulations for aqueous and organic slug is shown in Figure 1b. It shows three regions namely, recirculation region at the centre of the slug,

stagnant region where the liquid velocity is zero and film region. Similar type of circulations inside liquid slug of bubble train flow is shown by Gruber (2001). In this aqueous-organic slug flow, the aqueous phase acts as discrete phase while organic phase as continuous phase since it has less viscosity.

When there is no film, each slug moves with average flow velocity in the capillary. However in the presence of film (organic phase), the film separates aqueous slug from the wall and as a consequence, the aqueous slug moves with a velocity slightly greater than the average liquid velocity. This velocity can be calculated by assuming a fully developed laminar velocity profile in the capillary (Charles, 1963). The velocity of the slug is considered as maximum velocity (plug flow behavior) inside the capillary, and relates average velocity inside the capillary by the following equation:

$$V_s = \frac{2}{1+(R_s/R)^2} V_{av} \tag{2}$$

In order to calculate the mass transfer and rate of mixing inside the liquid slug, the recirculation time is an important parameter. Thulasidas et al (1997) defined the circulation time in bubble train flow as time for the liquid to move form one end of the slug to the other end. Likewise, in liquid-liquid slug flow, the dimensionless recirculation time can be written by the flowing equations:

Slug without film

$$t_{nofilm} = \frac{L\left(r^0\right)^2}{2\frac{L}{V_{av}}\int_0^{r^0} U(r) r dr} \tag{3}$$

Slug with film

$$t_{film} = \frac{L\left(r^0\right)^2}{2\frac{L}{V_s}\int_0^{r^0} U(r)\, r\, dr} \tag{4}$$

The radial position, r^0, is calculated by a velocity profile equation by putting the velocity equal to zero.

CFD Simulations

Problem Details and Solver

The problem was considered as two dimensional and the geometries of aqueous and organic phases were retrieved from the experimental results of Dummann et al (2003). In experiments, large aqueous hold up is used hence the results show aqueous phase with long slug which is several times the diameter of the capillary while the organic phase is with short slug. Since the slug size distribution analysis shows 5 % deviation from mean value, it was assumed that the slug geometry is constant for a given flow velocity. Each slug was considered separately as a single phase domain and solved for individual slug. The length of the aqueous phase domain for without and with film was same while the radius was changed with film thickness for aqueous slug with film. For organic slug without film, the domain was considered as a closed geometry while in the case of with film there was film flow inlet and outlet. The front and back interface of all slugs was assumed same (symmetric) at each flow velocity though there was convective flow in or out of the organic slug with film. The slug lengths used for simulation were 2.379 and 4.758 mm for aqueous phase while 0.561 and 1.122 mm for organic slug.

The inhouse developed open-source Finite Element CFD Tool, FEATFLOW, was used for simulations. This package solves the non-stationary incompressible Navier-Stokes equations:

$$\nabla \bullet u = 0,\ u_t - \nu \Delta u + u \bullet \nabla u + \nabla p = f, \qquad in\, \Omega \times [0,T] \tag{5}$$

The FEATFLOW package gives freedom to use two different approaches like a coupled approach and a projected approach to treat the discretized nonlinear system. The coupled approach couples velocity and pressure, promises best stability behavior but require largest numerical efforts while the projected solver decouples velocity and pressure, reduces the problem to the solution of a sequence of scalar problem (Turek, 1999). So in this case, the projected solver was used to simulate the flow field.

Numerical Grid and Boundary Conditions

In this study, the geometry considered is shown in Figure 1, with front interface being concave while back interface being convex for aqueous slug and vice a versa for organic slug. The structured two-dimensional coarse grid was generated with the help of in house developed Design and Visualization Software Resource (DeViSoR 2.1). The grid was refined near the wall and corner of the geometry for improving the resolution. The boundary conditions of aqueous phase are the same for slug without and with film. For aqueous slug and organic slug without film, since there was no inflow and outflow, Dirichlet type boundary condition was used. In organic phase domain with film, there was film inlet and outlet, Neumann type boundary condition was used. The negative x-velocity was given to the capillary wall which moved the capillary wall in negative direction while the slug was stationary. The other velocities like film velocity and interface velocities were defined relatively.

Solution and Postprocessing

Initially the simulations were carried out in order to make the solution grid independent using different levels of refinement. Stationary flow fields were achieved with equidistant time stepping of 0.01 and total time of 30 sec for each slug. Similarly equidistant time stepping of 0.25 was used for visualization of General Mesh Viewer (GMV) outputs. The GMV outputs were taken with the same level of refinement. The Sun-Fire-880 computer system with 900 MHz Sparcv9 processor was used for simulation. The total time required for simulation was 1530 and 400 for aqueous (L = 2.379 mm) and organic (L = 0.561 mm) respectively.

Particle Tracing

Looking from the transport phenomenon point of view, it is crucial to know how and where circulation develops and where regions of stagnant flow are located. Here we show a method that can solve this problem called particle tracing. It is a method to visualize the material transport caused by a given stationary or instationary flow. This converts a eulerian description of a flow into the corresponding lagrangian description. The difference is that it can only be done for some selected particle locations and not for the whole domain. Practically we define some particle sources that generate virtual massless particles once or on a regular basis and follow the path in the given flow field over time.

We have developed the algorithm called GMVPT (General Mesh Viewer Particle Tracing). It doesn't do its own flow simulation but imports flow fields from a series of GMV files generated by FEATFLOW. The domain description was given by a coarse grid and its refinements up to the level used by the GMV files. These were used to build up a hierarchical searching structure to determine in which cell each particle resides. Initially only the position

of a particle was given. The velocity of the flow at that position is in most cases not directly given and has to be interpolated from the values given in the grid nodes. By this information and the time step, we could determine the new position by the following simple relation:

$$\tilde{Z} = Z + \Delta t u_P \tag{6}$$

First we had to determine in which cell that particle was and which node data we had to use for the interpolation. This was done by using the multilevel structure of the grids as shown in Figure 2. Ideally full searches were done only on the coarse grid level and then only for the cells that were generated by refining the found cells were looked at. But this only works with cell hierarchies which have the property that all generated cells are included in the cells they are generated from. For boundary cells this is not always true. Cells that are outside of their parent cell have because of this to be checked separately for each refinement level. For complicated domains with complex coarse grids, this method looses some of its advantages and it is planned to replace this method later by a quad tree based approach. If no cell can be determined to contain the particle, it will be considered outside of the domain and deleted. After we have determined a cell that contains the particle, a Newton based approach was used to reverse project the particle to the standard cell. There we perform a bilinear interpolation of the velocities (and other data fields) that was given in the corners of the standard cell. This approach works also for 3D where we can have hexahedral cells with non flat sides.

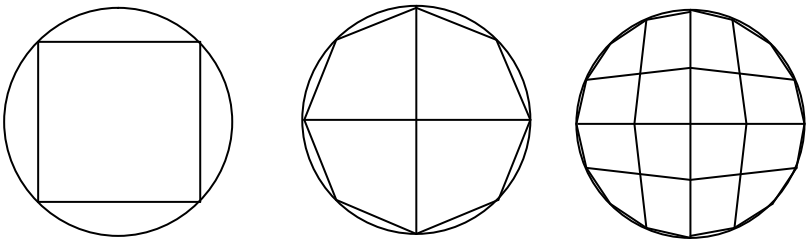

Figure 2: Cell refinement

At this point the flow fields for instationary flows were not interpolated and used piecewise constant in time. The simulations were carried out with the result obtained by previous CFD simulations. The meshes with different level of refinement were generated with the help of in-house developed graphical preprocessing tool, TRIGEN2D. It is the tool for 2D coarse triangulations and to write the corresponding data in some special format onto hard disc. We inserted the rectangular area of tracers with a constant frequency to simulate a constant stream of particles at various operating conditions.

Results and Discussion

Velocity Profile

The counters of simulated x-directional velocity in slug (L > D) without film for aqueous and organic slug are shown in Figure 3a. As can be seen, maximum velocity at the center and minimum velocity at the wall, showing fully developed parabolic (Poiseuille) profile, given by the following equation,

$$\frac{U(r)}{V_{av}} = 1.5\left(1 - \frac{r^2}{R^2}\right) - 1 \qquad (7)$$

Similar type of study was made by Thulasidas et al. (1997) in gas-liquid flow through circular and square cross section capillaries. This parabolic profile is bidirectional showing maximum velocity at the centre of the slug, zero velocity at some radial position r^0 and negative velocity at the wall surface (see Figure 3b). The bidirectional profile is due to the closed geometries which become flat with decrease in the flow velocity. In the case of short slugs (like organic slug, L = 0.561 mm) with length is not long as compared to the diameter of the capillary, the profile observed was quantitatively different showing not fully developed flow. In this case,

dead zones rather than recirculation were observed. In some simulations, it shows that the front part of the slug has dead zones and the back part has circulation at the corner only. Increase in the length of the slug, the velocity profile was approached like Parabolic (Poiseuille) profile. In the case of slugs with film, the aqueous slug has same parabolic profile while in organic slug the parabolic profile is slightly disturbed near the interface due to film inlet and outlet but fully developed profile was observed at the centre of the slug. At the centre of the slug, the same velocity profile like slug without film was observed since the film thickness is very less as compared to the diameter of the slug.

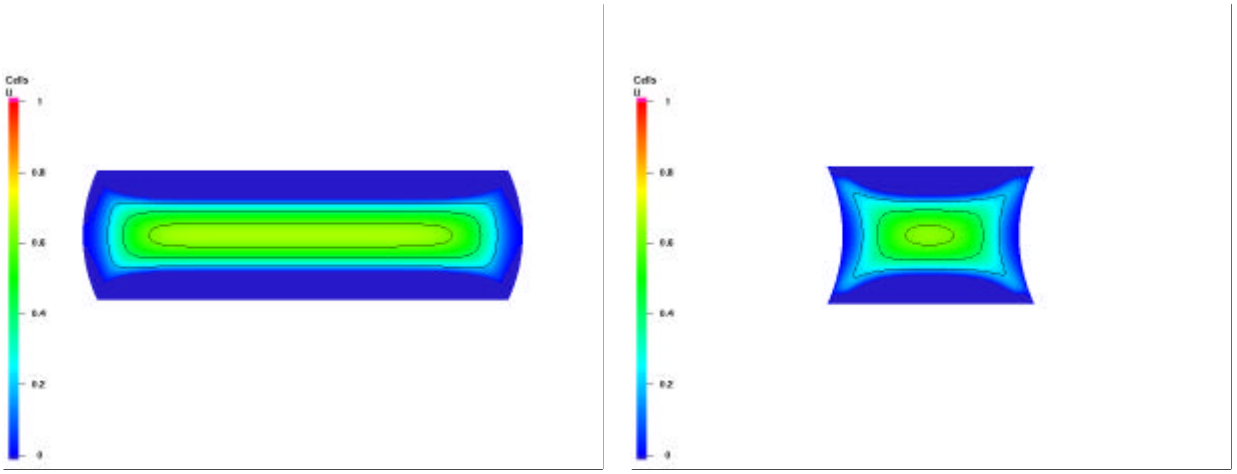

Figure 3a: Contours of velocity in x-direction (u) of aqueous and organic slug respectively

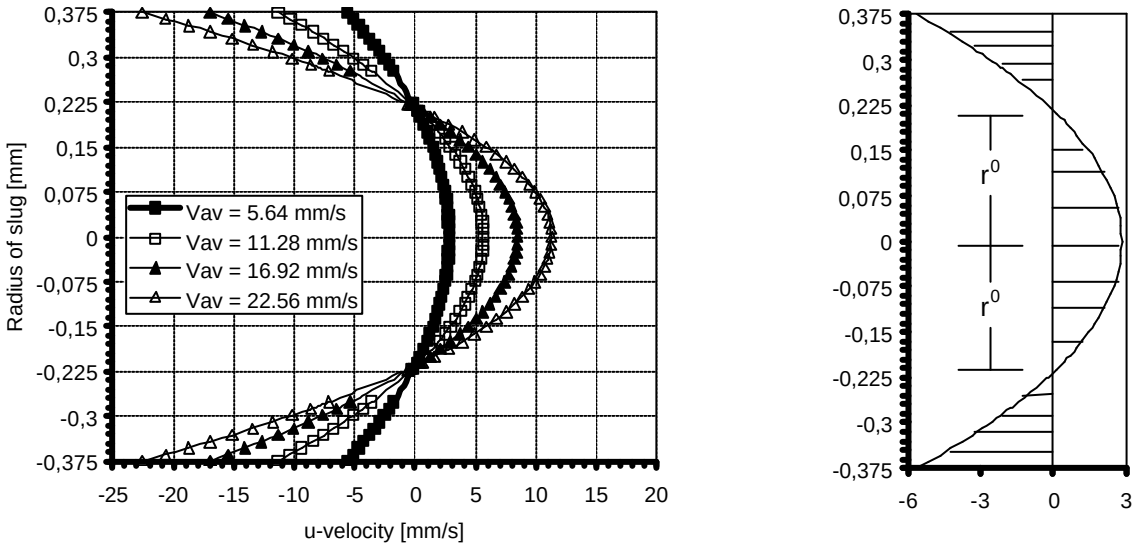

Figure 3b: Parabolic velocity profile inside the slug.
(Aqueous slug, L = 2.379 mm, D = 0.75 mm)

Internal Recirculations

In slug flow reactor, when the solute diffuses through the interface from one slug to the other, it circulates inside the slug and convective mass transfer takes place. Here the convective mass transfer depends on the intensity of internal circulations while diffusion depends on the intensity of circulations inside both slugs. The contours of internal circulations (velocity vector magnitude) inside the aqueous and organic slug showing circulations and stagnant region (zero cell vector magnitude) are shown in Figure 4. These circulations were observed at all flow velocities. Similar type of recirculations inside the discrete liquid drop in a slit type were presented by Handique and Burns (2001) and studied the convection and diffusion dominated mixing strategy of solute in a moving discrete drop.

The recirculations are around the two stagnant regions (see Figure 1b) showing intensity of recirculation is more at the centre of the slug and in between two stagnant regions. The velocity inside the slug is zero at this stagnant region and the radial position was calculated by equating u(r) equal to zero in velocity profile equation. This dimensionless radial distance as a function of average flow velocity is plotted in Figure 5. As can be seen, at low flow velocity the stagnant region is at half of the length of the slug but with further increase in velocity (~50 mm/s), the stagnant region shifts towards the back interface (upstream) of the slug. The liquid circulate around the stagnant region hence the intensity of circulation is more towards the back interface. In the case of slug without film, with increasing length of the slug, the stagnant region shifts more towards the upstream. The same behavior was observed for aqueous slug with film also. But for organic slug with flow, since there is inflow and outflow, the stagnant region as at the centre of the slug at all flow velocities, showing that the intensity of recirculations is maximum at the centre.

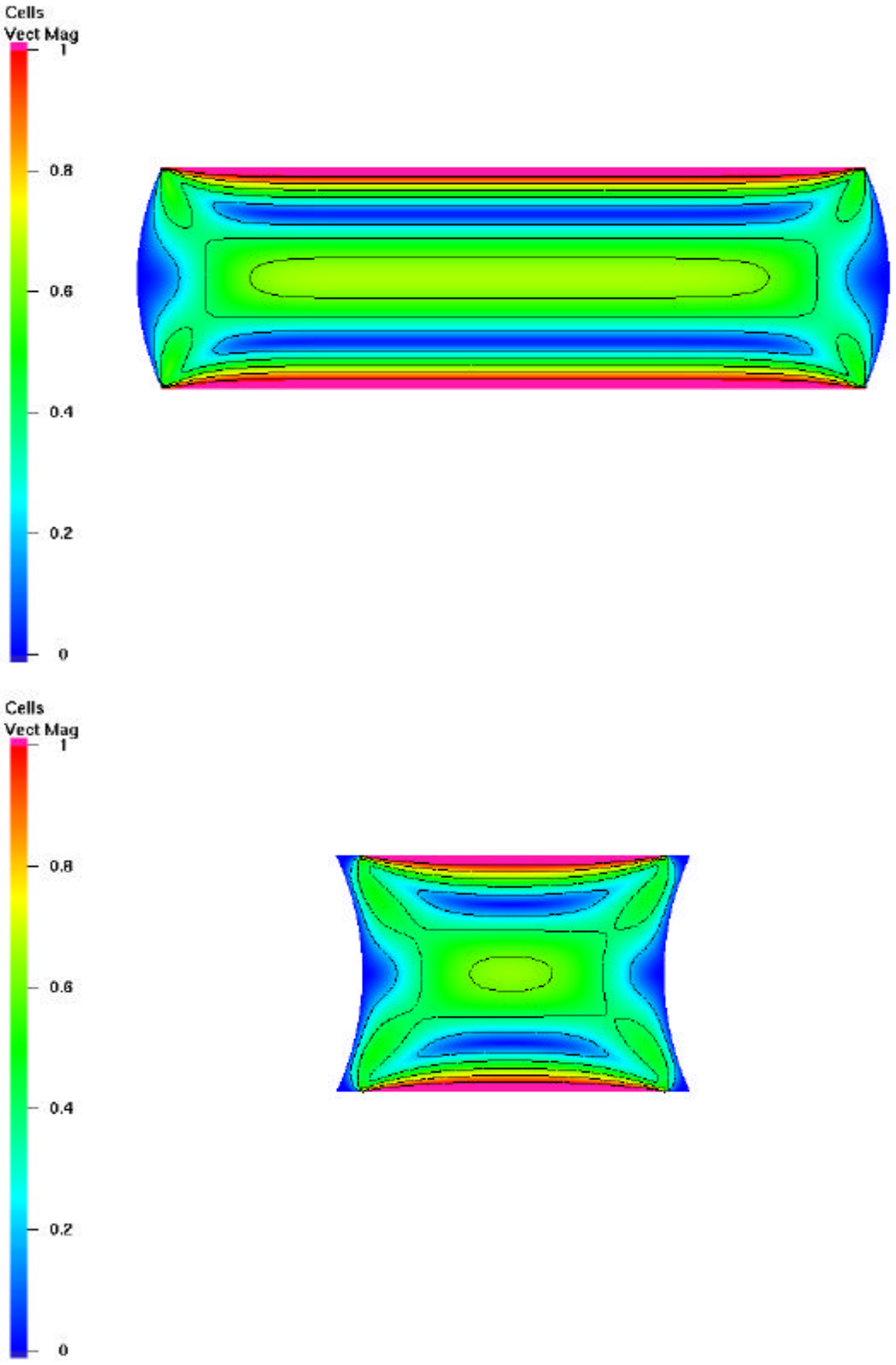

Figure 4. Internal circulations inside the aqueous and organic slug respectively

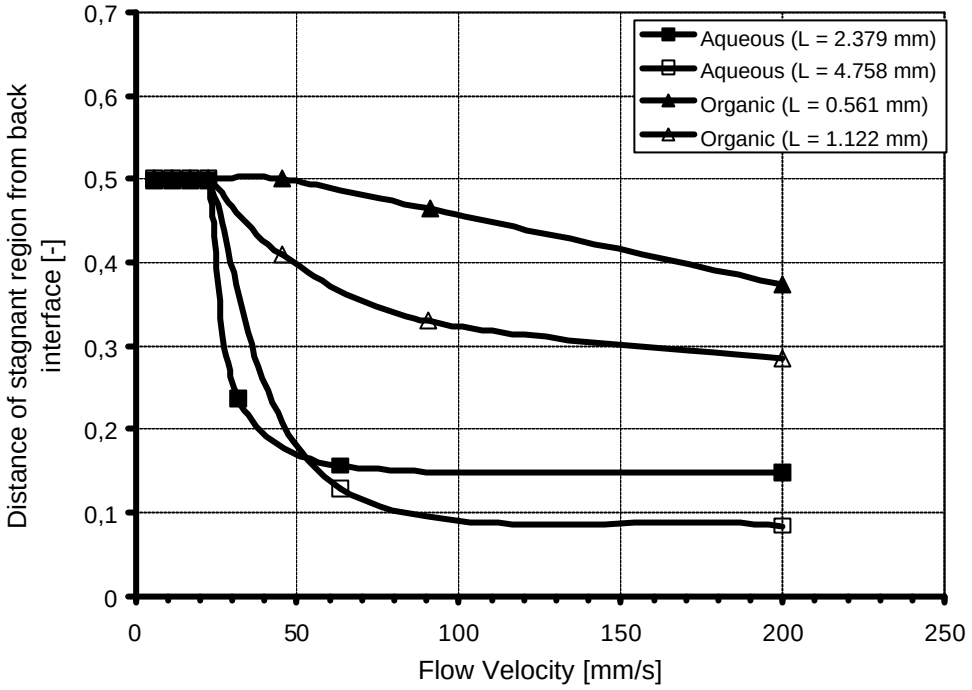

(a)

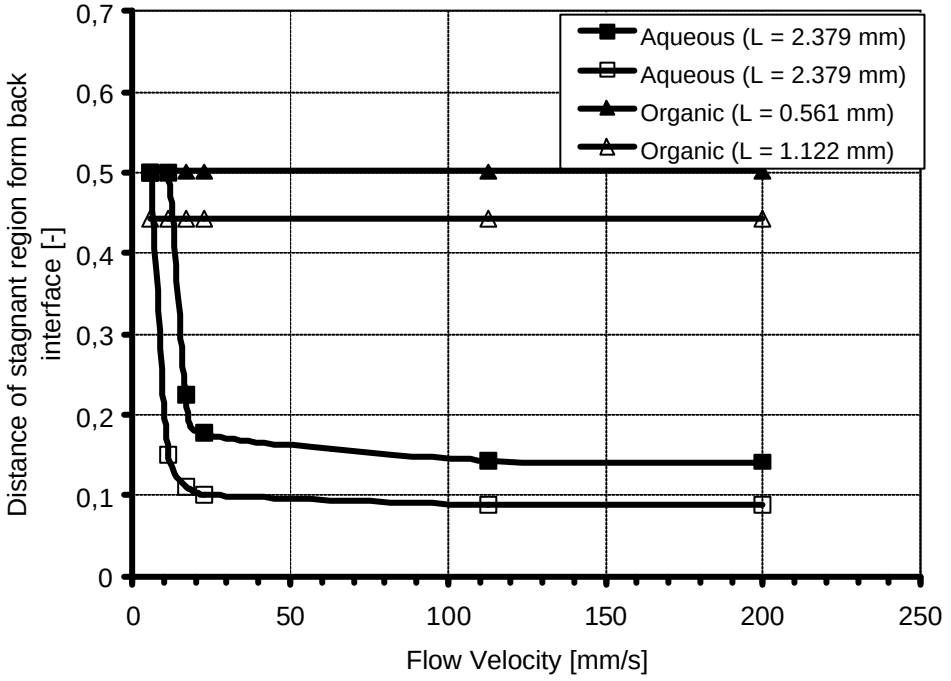

(b)

Figure 5: Distance of centre of stagnant region from the back interface for slugs without and with film respectively

The circulation time inside the slug is calculated from simulated results (Equation 3 and 4) and plotted as a function of average flow velocities in Figure 6. Thulasidas et al (1997)

reported recirculation time in gas-liquid flow with film showing that at low capillary number the recirculation time inside the liquid slug has no effect but increases at high capillary number (~ 0.1). In case of slug without film, for a slug with sufficient length (L>D), the flow velocity has no significant effect on circulation time. The circulation time is constant in between 3 to 4 which indicates that a typical particle inside the slug will move from one end of the slug to other end during the time the slug travel a distance of 3 to 4 times its length. For a slug with length less than the diameter of the slug (see organic slug with L = 0.5616 mm in Figure 7), at low liquid velocity the circulation time was constant, but with increase in the flow velocity, circulation time decreases and again remains constant. It shows that at low flow velocity, the liquid circulate slowly and the circulations increases with increase in flow velocity upto 80 mm/s but further increase in velocity has no effect on recirculation time. In film flow, for aqueous slug the circulation time is larger than the case of without film due to the decrease in the diameter of the slug and increase in slug velocity. It also decreases with increase in the flow velocity. For organic slug, the circulation time is constant at all flow velocities since there was film inflow and outflow as well.

Particle Tracing

The simulations with 2000 macro time steps and duration of 0.01 for both the slugs at different tracer block locations were carried out. The internal circulations inside aqueous and organic slug by particle tracing observed at different time for a flow velocity of 5.64 mm/s are shown in Figure 7. As can be seen, the rectangular block with 100x100 particles is located along the axis near to the back interface at time zero. With increase in time, the particles move along the flow and reach the other end of the slug within 2 sec for aqueous slug and 1 sec for organic slug. The simulations with blocks of height equal to the diameter of the slug clearly show the circulations and the stagnant region inside the slug. The particle in the stagnant

region stays at the same position while the other particles move around them showing recirculations. Thus, the particle tracing shows quantitative prediction of internal circulations inside the liquid slugs.

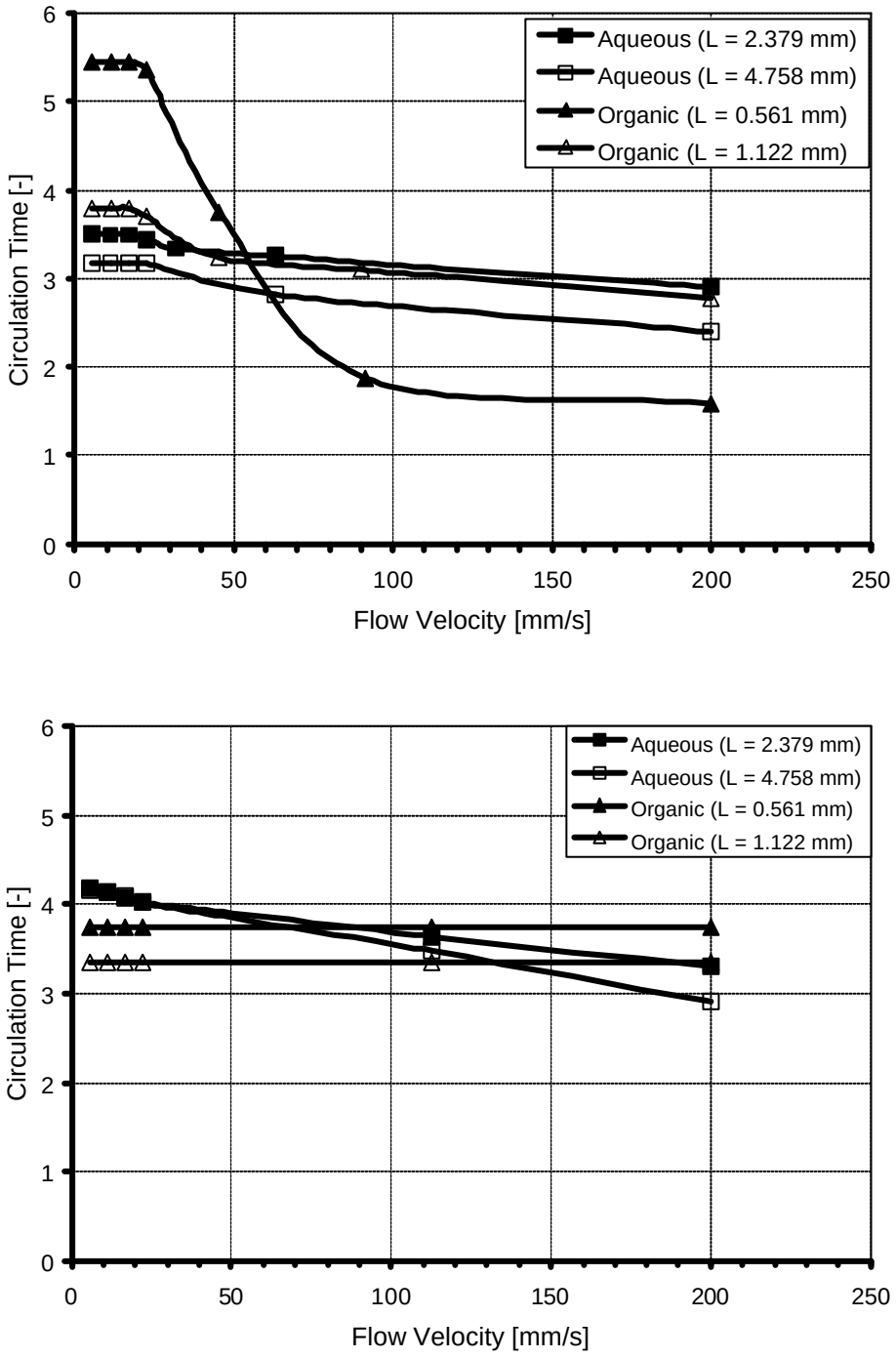

Figure 6: Circulation time inside the liquid slug with respect to the average flow velocity.

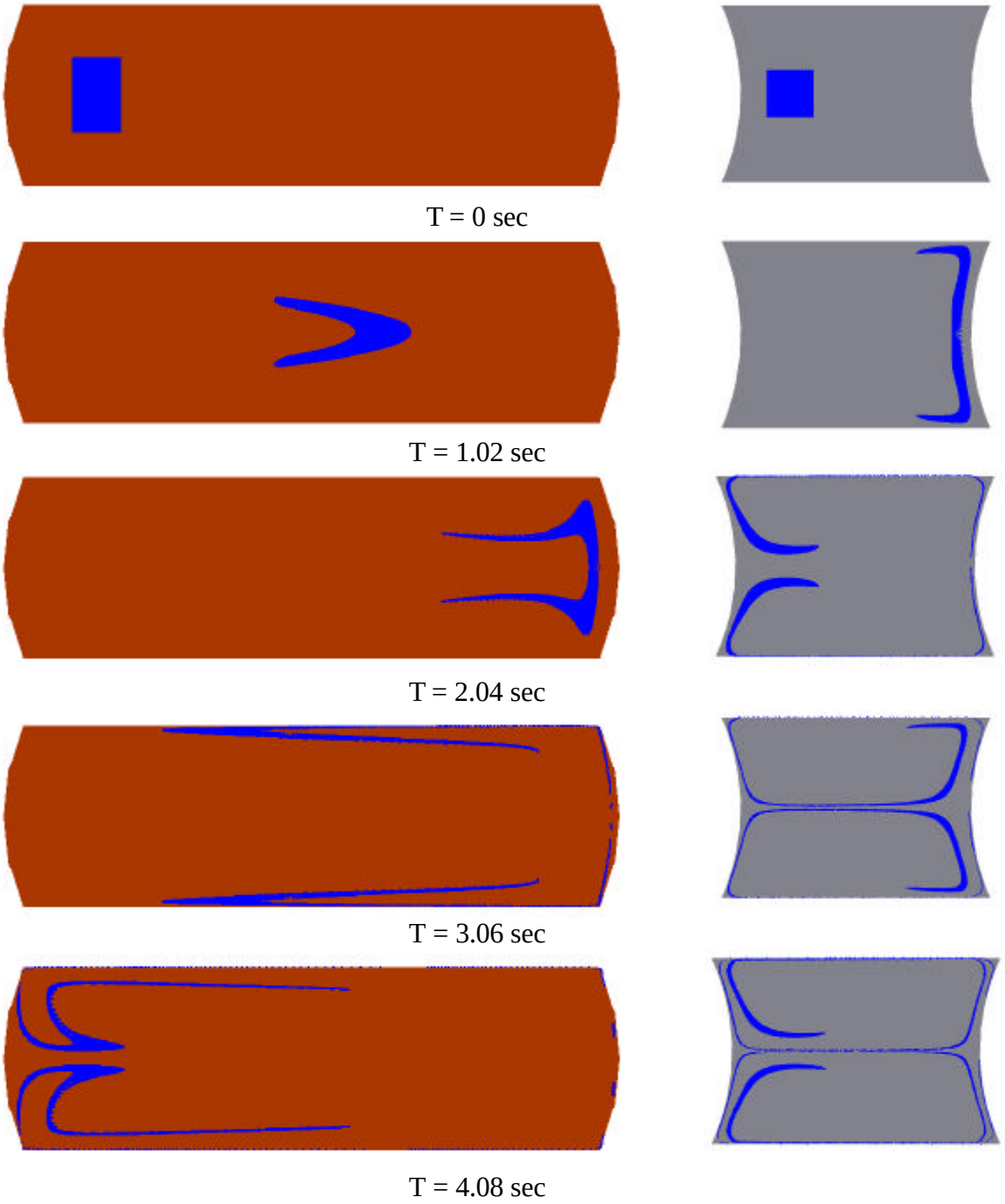

Figure 7: Internal circulations by particle tracing in aqueous and organic slugs respectively.
(V_{av} = 5.64 mm/s, D = 0.75 mm)

Conclusion

The effect of different flow velocities on the velocity profile and internal circulations has been studied with the help of CFD. A particle tracing algorithm was developed to visualize the flow patterns inside the slug. The simulated results show that the position of the stagnant region changes with change in flow velocity. At low flow velocity and slug with sufficient length, the flow has no significant effect on the circulation time inside the slug but with further increase in flow velocity the circulation time decreases. The developed particle tracing algorithm gives qualitative information about the circulations and stagnant region. In the future work, free surface CFD methodology will be developed and physical experiments will be carried out for internal circulations.

Notations

C_a	Capillary number [-]
h	Film thickness [mm]
L	Length of slug [mm]
R	Radius of capillary [mm]
R_S	Radius of slug [mm]
r	Radial position [mm]
r^0	Radial position of stagnant region [mm]
$U(r)$	Velocity inside the slug at radial position r [mm/s]
V_{av}	Average flow velocity [mm/s]
V_S	Slug velocity [mm/s]
V_P	Velocity of particle [mm/s]
t	Circulation time [-]
Z	Initial position of the particle [mm]
$\tilde{Z}$	Position of particle after time Δt [mm]

References

Bercic Gorazd & Pinter Albin (1997), The role of gas bubbles and liquid slug lengths on mass transport in the Taylor flow through capillaries, *Chemical Engineering Science, 52 (21/22), 3709-3719*.

Bico, J., & Quere, D. (2000), Liquid trains in a tube, *Europhysics Letters, 51(5), 546-550*.

Bothe Dieter., Koebe Mario., Wielage Kerstin & Warnecke Hans-Joachim. (2003), VOF-simulations of mass transfer from single bubbles and bubble chains rising in aqueous solutions, *Proceedings of FEDSM'03: 4th ASME_JSME Joint Fluids Engineering Conference, Honolulu, Hawaii, USA.*

Burns, J. R., & Ramshaw, C. (1999), Development of a microreactor for chemical production, *Trans IChemE, 77(A), 206-211*.

Burns, J. R., & Ramshaw, C. (2001), The intensification of rapid reactions in multiphase systems using slug flow in capillaries, Lab on Chips, 1, 10-15.

Charles, M. E. (1963), The pipeline flow of capsules, Part 2: The concept of capsule pipelining, *The Canadian Journal of Chemical Engineering, 46-51*.

Dummann Gerrit., Quittmenn Ulrich., Gröschel Lother., Agar David, W., Wörz Otto, & Morgenschweis Konard (2003), The capillary-microreactor: a new reactor concept for the intensification of heat and mass transfer in liquid-liquid reactions, *Catalysis Today, 79-80, 433-439*.

Elperin, T., & Fominykh, A. (1998), Mass transfer during gas absorption in a vertical gas liquid slug flow with small bubbles in liquid plugs, *Heat and Mass Transfer, 33, 489-494*.

GMV (General Mesh Viewer), *user manual, Release 2.2, 2000. (http://www-xdiv.lanl.gov/XCM/gmv/GMVHome.html).*

Gruber Rainer (2001), Radial mass transfer enhancement in bubble train flow, *Ph.D. Thesis, RWTH Aachen, Germany.*

Handique, K. & Burns, M. A. (2001), Mathematical modeling of drop mixing in a slit type microchannel, Journal of Micromechanics and Microengineering, 11, 548-554.

Harries, N., Burns, J. R., Barrow, D. A., & Ramshaw, C. (2003), A numerical model for segmented flow in a microreactor, *International Journal of Heat and Mass Transfer, 46, 3313-3322*.

Hodgson, G. W., & Charles, M. E. (1963), The pipeline flow of capsules, Part 1: Theoretical analysis of the concentric flow of cylindrical forms, *The Canadian Journal of Chemical Engineering, 43-45*.

Kreutzer Michiel (2003), Hydrodynamics of Taylor flows in capillaries and monolith reactors, *Ph.D Thesis, Delft University Press, Netherlands.*

Kunugi Tomoaki., Banat Mohamed & Ose Yasuo (1999), Slug –plug flow analyses of stratified multiphase flows in a horizontal duct, *7th International Conference on Nuclear Engineering Tokyo, Japan.*

Mishima K., & Hibiki T. (1996), Some characteristics of air-water two-phase flow in small diameter vertical tubes, *International Journal of Multiphase Flow, 22, 703–712*.

Paglianti, A., Giona, M., & Soldati, A. (1996), Characterization of subregimes in two-phase slug flow, *International Journal of Multiphase Flow, 22 (4), 783-796.*

Piarah, W. H., Paschedag, A. & Kraume, M. (2001), Numerical simulation of mass transfer between a single drop and an ambient flow, *AIChE Journal, 47 (7), 1701-1704.*

Shearer, C. J. (1973), Mixing of highly viscous liquids: flow geometries for streamline subdivision and redistribution, *Chemical Engineering Science, 28, 1091-1098.*

Simmons, M.J., Wong, D.C.Y., Travers, P.J., & Rothwell J.S. (2003), Bubble behaviour in three phase capillary microreactors, *International Journal of Chemical Reactor Engineering, 1, A (30)*.

Taha, T., & Cui, Z. F. (2004), Hydrodynamics of slug flow inside the capillaries, *Chemical Engineering Science, 59, 1181-1190.*

Thulasidas, T.C, Abraham, M. A., & Cerro, R. L. (1995), Bubble train flow in capillaries of circular and square cross section, *Chemical Engineering Science, 50 (2), 183-199*.

Thulasidas, T.C., Abraham, M. A., & Cerro, R. L. (1997), Flow pattern in liquid slugs during bubble train flow inside capillaries, *Chemical Engineering Science, 52 (17), 2947-2962.*

Triplett, K. A., Ghiaasiaan, S. M., Abdel-Khalik, S. I., & Sadowski, D. L. (1999), Gas-Liquid two-phase flow in microchannels Part I: two-phase flow patterns, *International Journal of Multiphase Flow, 25, 377-394*.

Turek, S (1999), Efficient Solvers for Incompressible Flow Problems: An Algorithmic and Computational Approach, *Springer-Verlag, Heidelberg.*

Waheed Adekojo, M., Henschke Martin & Pfennig Andreas (2002), Mass transfer by free and forced convection from single spherical liquid drops, *International Journal of Heat and Mass Transfer, 45, 4507-4514.*

Wolffenbuttel Brigitte, Monolithic reactors for liquid-liquid and gas-liquid-liquid applications: Hydrodynamics and Mass Transfer, *Ph.D Thesis, Delft University of Technology, Netherlands.*

Zou Baisheng, Dudukovic Milord, P., & Mills Patrick, L. (1993), Modeling of evacuated pulse micro-reactors, *Chemical Engineering Science, 48 (13), 2345-2355.*